AJNR Am J Neuroradiol 20:487–494, March 1999

Angiographic Abnormalities in Progressive Multifocal Leukoencephalopathy: An Explanation Based on Neuropathologic Findings

Peter Kim Nelson, Lynette T. Masters, David Zagzag, and Patrick J. Kelly

BACKGROUND AND PURPOSE: **Progressive multifocal leukoencephalopathy (PML) is typically occult at angiography and fails to enhance on MR images. After observing angiographic abnormalities characterized by arteriovenous shunting and pathologic parenchymal blush in patients with AIDS-related PML, often in the absence of contrast enhancement on MR images, we hypothesized that there might be distinct changes in the cerebral microvasculature that account for the reduction in vascular transit time (arteriovenous shunting) in the absence of blood-brain barrier dysfunction.**

METHODS: **The imaging studies and neuropathologic specimens of six patients with biopsy-proved PML were reviewed retrospectively. In all patients contrast-enhanced MR imaging and CT, followed by cerebral angiography, were performed before stereotactically directed biopsy. The angiograms were evaluated for the presence of vascular displacement, pathologic parenchymal blush, arteriovenous shunting, and neovascularity. The CT and MR studies were reviewed for the presence of enhancement of the PML lesions. Biopsy specimens were examined for the presence of necrosis, perivascular inflammation, and neovascularity.**

RESULTS: **All patients had oligodendrocytic intranuclear inclusions diagnostic of PML, together with perivascular inflammation and neovascularity to a varying extent; no other neuropathologic processes were identified. Angiographic abnormalities, characterized by a pathologic parenchymal blush and arteriovenous shunting, were identified in four of the six patients. In only one of these cases, however, was abnormal enhancement identified on cross-sectional imaging studies (MR and CT), and this patient had florid perivascular inflammatory infiltrates histologically.**

CONCLUSION: **The pathologic parenchymal blush and arteriovenous shunting seen angiographically in some patients with PML reflect small-vessel proliferation and perivascular inflammatory changes incited by the presence of the JC virus in infected oligodendrocytes.**

Progressive multifocal leukoencephalopathy (PML) is a demyelinating disease of the brain caused by infection of oligodendrocytes by a papovavirus (the JC virus) (1). It occurs in individuals with impaired cell-mediated immunity, and was initially described in patients with chronic hematologic malignancies (lymphoma and chronic lymphocytic leukemia) (2, 3) and immunosuppression due to other causes (eg, tuberculosis, sarcoidosis, iatrogenic causes) (1, 3, 4). PML occurs in 3.8% to 7% of persons with AIDS (1, 4–7), and is the AIDS-defining illness in about 1% of cases (8). PML is usually diagnosed after the onset of focal neurologic deficits or a deterioration in cognitive function, and almost always follows a relentless course, with death typically occurring within 9 months of the onset of symptoms (2–7).

The appearance of PML on cross-sectional imaging studies is well described; the angiographic findings are less well characterized. We report the spectrum of angiographic findings in six patients with biopsy-proved PML, and compare these with the cross-sectional and neuropathologic findings.

Received April 21, 1998; accepted after revision November 2.

Presented at the annual meeting of the American Society of Neuroradiology, Toronto, Canada, May 1997.

From the Neurointerventional Service, Department of Radiology (P.K.N., L.T.M.), the Division of Neuropathology, Department of Pathology (D.Z.), the Department of Neurosurgery (D.Z., P.J.K.), and the Kaplan Comprehensive Cancer Center (D.Z., P.J.K.), New York University Medical Center, New York, NY.

Address reprint requests to Peter Kim Nelson, MD, Neurointerventional Service, Department of Radiology, New York University Medical Center, 560 First Ave, New York, NY 10016.

Imaging findings in six patients with biopsy-proved progressive multifocal leukoencephalopathy

Patient	Age (y)/Sex	Imaging Findings		
		CT	MR Imaging*	Angiography
1	F/40	L cerebellar hypodensity, mild mass effect, enhancing	L brachium pontis mass, mild mass effect, enhancing	Mass effect, A/V shunting, blush
2	M/50	R frontal hypodensity, no mass effect, no enhancement	R frontal mass, no mass effect, no enhancement	No mass effect, A/V shunting, blush
3	M/40	Bifrontal hypodensities (L > R), no mass effect, no enhancement	Bifrontal masses (L > R), mild mass effect, no enhancement	Mass effect, A/V shunting, blush
4	M/47	L frontoparietal hypodensity, no mass effect, no enhancement	L frontoparietal mass, no mass effect, no enhancement	Mass effect, A/V shunting, blush
5	M/41	L frontal and parietal hypodensities, no mass effect, no enhancement	L frontal and parietal masses, corpus callosum and R hemispheric lesions, no mass effect, no enhancement	No mass effect, no A/V shunting, no blush
6	M/48	Multiple bilateral subcortical hypodensities, no mass effect, no enhancement	Multiple bilateral subcortical and cortical lesions, no mass effect, no enhancement	No mass effect, no A/V shunting, no blush

Note.—A/V indicates arteriovenous.

* All lesions were hypointense relative to normal white matter on short TR/TE images and hyperintense on long TR/TE images.

Methods

In a retrospective review we identified nine patients with a biopsy-proved diagnosis of PML. Of this group, six patients underwent contrast-enhanced CT and MR imaging, as well as cerebral angiography, prior to stereotactically directed lesion biopsy. These patients form the basis of this report.

The study group included five men and one woman, ranging in age from 40 to 50 years (mean age, 44 years). Four of the patients were known to be HIV positive for periods ranging from 1 to 10 years; one patient (case 5) had a preexisting diagnosis of AIDS (as defined by the Centers for Disease Control, Atlanta, GA). In the remaining two cases, the positive HIV status was established during assessment of new onset of neurologic symptoms. Risk factors for HIV infection were present in all the male patients; no obvious risk factor for HIV infection was identified in the female patient. The absolute CD4 T lymphocyte count at the time of admission to the hospital was available for two patients and the CD4:CD8 ratio was available in one additional case. Patient 5 had an absolute CD4 count of 72 μL (normal range, 480–1367 μL) and patient 6 had a value of 6 μL. In patient 1 there was reversal of the normal CD4:CD8 ratio (the absolute cell count was not available in this patient). Presenting neurologic signs and symptoms included progressive hemiparesis in two cases, dysphasia in two, incoordination and ataxia in one, and homonymous hemianopsia in two; three patients also had mild cognitive impairment. Neurologic symptoms and signs correlated closely with the anatomic location of lesions. The time interval from the onset of neurologic symptoms to biopsy ranged from 1 to 12 weeks (mean, 5.7 weeks).

The six patients underwent MR imaging, CT, and cerebral angiography after the placement of a stereotactic head frame. These imaging studies are part of the standard protocol for patients referred for stereotactic biopsy or stereotactic volumetric resection of intracranial masses at our institution. MR imaging was performed on a 1.5-T system and consisted of contrast-enhanced axial T1-weighted (600/14/2 [TR/TE/excitations]) sequences, fast spin-echo T2-weighted (3400/17,119/1) sequences, and T1-weighted volumetric gradient-echo (11.4/4.4/1) sequences. CT was performed after the administration of 150 mL of 60% nonionic contrast material. Digital subtraction cerebral angiography was performed after selective catheterization of the pertinent internal carotid and/or vertebral arteries, and in each case followed the cross-sectional imaging studies. In each patient, all imaging studies were performed on the same day, and were followed within 24 hours by biopsy or resection of the lesion. Informed consent was obtained in all cases.

The imaging studies were reviewed retrospectively by two neuroradiologists. The angiograms were analyzed for the presence of vascular displacement, pathologic parenchymal blush, and evidence of arteriovenous shunting. The MR and CT studies were analyzed to determine the number and distribution of lesions and, in particular, whether contrast enhancement was present.

In each patient, multiple (three to six) stereotactically directed biopsy specimens were obtained from the lesions identified on cross-sectional imaging studies. These were all reviewed retrospectively by one neuropathologist, who was blinded to the radiologic findings. Biopsy samples were analyzed for the presence of oligodendroglial intranuclear inclusions, necrosis, gliosis, perivascular infiltrates, capillary density, and neovascularity.

Results

The findings on CT, MR, and angiographic studies are summarized in the Table. There were no complications related to the angiography or cross-sectional imaging studies.

In five patients, lesions were restricted to the supratentorial compartment, and, in one case, disease was confined to the posterior fossa. MR imaging was superior to CT in defining the extent of the foci of PML and revealed additional white matter disease in one patient (case 5), which consisted of abnormal signal in the corpus callosum and right hemispheric white matter. In patient 1, the focus of PML in the left brachium pontis enhanced on both MR and CT examinations (Fig 1A and B).

Angiographic abnormalities, characterized by varying combinations of abnormal parenchymal blush, arteriovenous shunting, and vascular displacement, were identified in four of the six patients (cases 1–4) (Figs 1–3). Typically, the parenchymal blush developed in the early to mid-arterial phase of the angiogram and persisted into the venous phase and was associated with arteriovenous

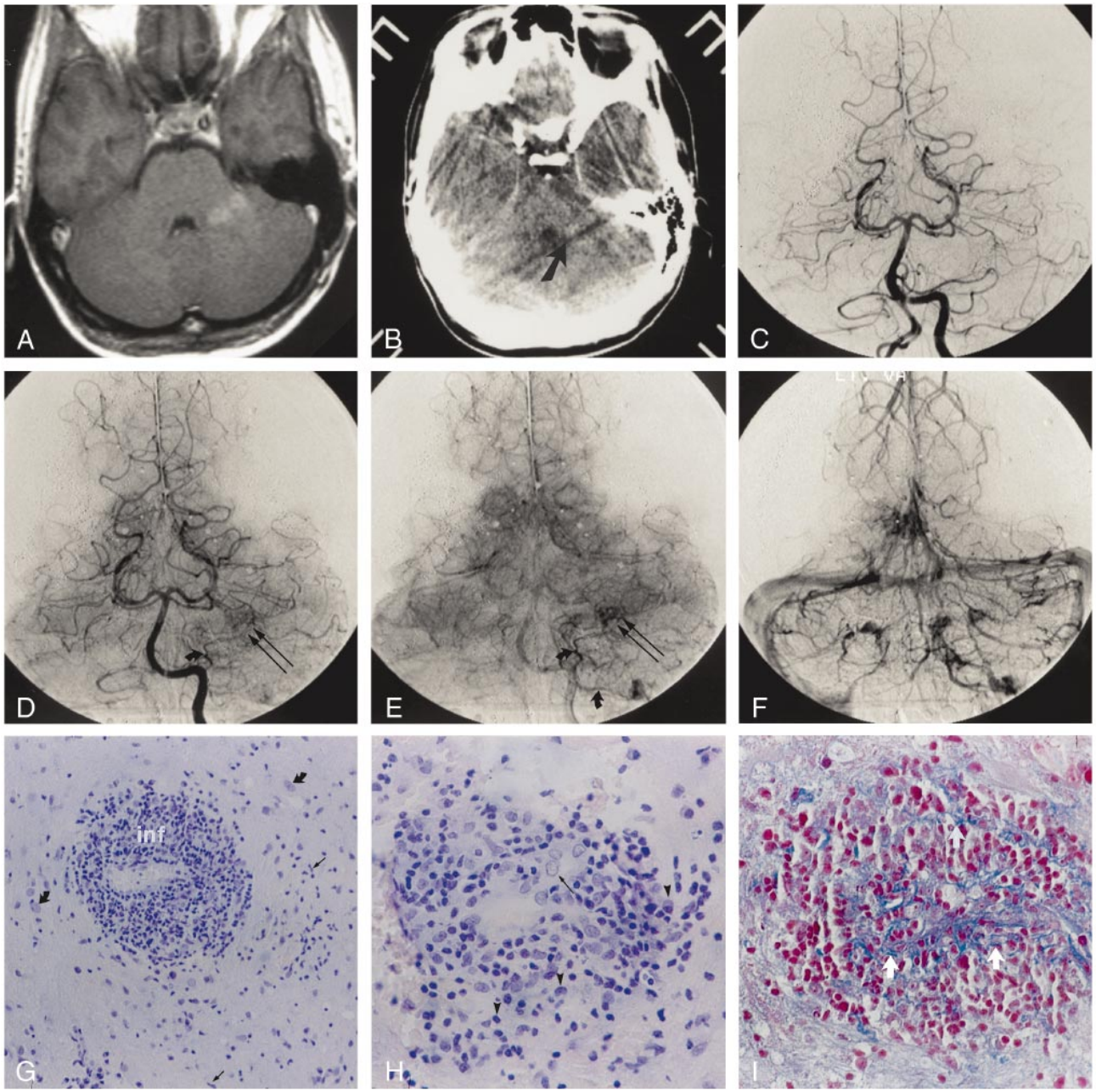

FIG 1. Patient 1.

A, Contrast-enhanced axial T1-weighted MR image (600/14/2) shows an enhancing lesion in the left brachium pontis.

B, Contrast-enhanced CT scan at the same level as the MR image. Although there is considerable streak artifact in the posterior fossa, there is an enhancing lesion in the left brachium pontis (*arrow*) corresponding to that identified on the MR image.

C–F, Early arterial (*C*), mid-arterial (*D*), capillary (*E*), and venous (*F*) phase images from the left vertebral artery stereo angiogram (anteroposterior projection) show an abnormal parenchymal blush (*double arrows*) in the left cerebellar hemisphere corresponding to the lesion seen on the CT and MR studies. There is arteriovenous shunting with early opacification of the left lateral recess and cerebellomedullary veins (*curved arrows*), which empty into the left sigmoidal sinus.

G, Histopathologic specimen shows exuberant perivascular inflammation (*inf*). The surrounding tissue shows gliosis (*curved arrows*) and microglial activation (*straight arrows*) (hematoxylin-eosin, original magnification ×100).

H, Higher-power view shows the mixed population of inflammatory cells, including lymphocytes, monocytes, and plasma cells (*arrowheads*). Note the plumping of the endothelial cells (*arrow*) (hematoxylin-eosin, original magnification ×200).

I, Azocarmine stain of tissue specimen in *G* shows reduplication of the basal lamina (*arrows*), seen as a fine connective tissue network (azocarmine stain, original magnification ×200).

shunting. The blush corresponded in location to the PML lesions seen on cross-sectional images. Vascular displacement was seen in three patients. In only two patients (cases 5 and 6) were the angiograms normal in appearance (Fig 4).

In each case, stereotactically directed biopsies revealed oligodendrocytic intranuclear inclusions diagnostic of PML, together with a variable degree of gliosis. Perivascular inflammatory infiltrates and sprouting angiogenesis (Fig 3F) were seen to a

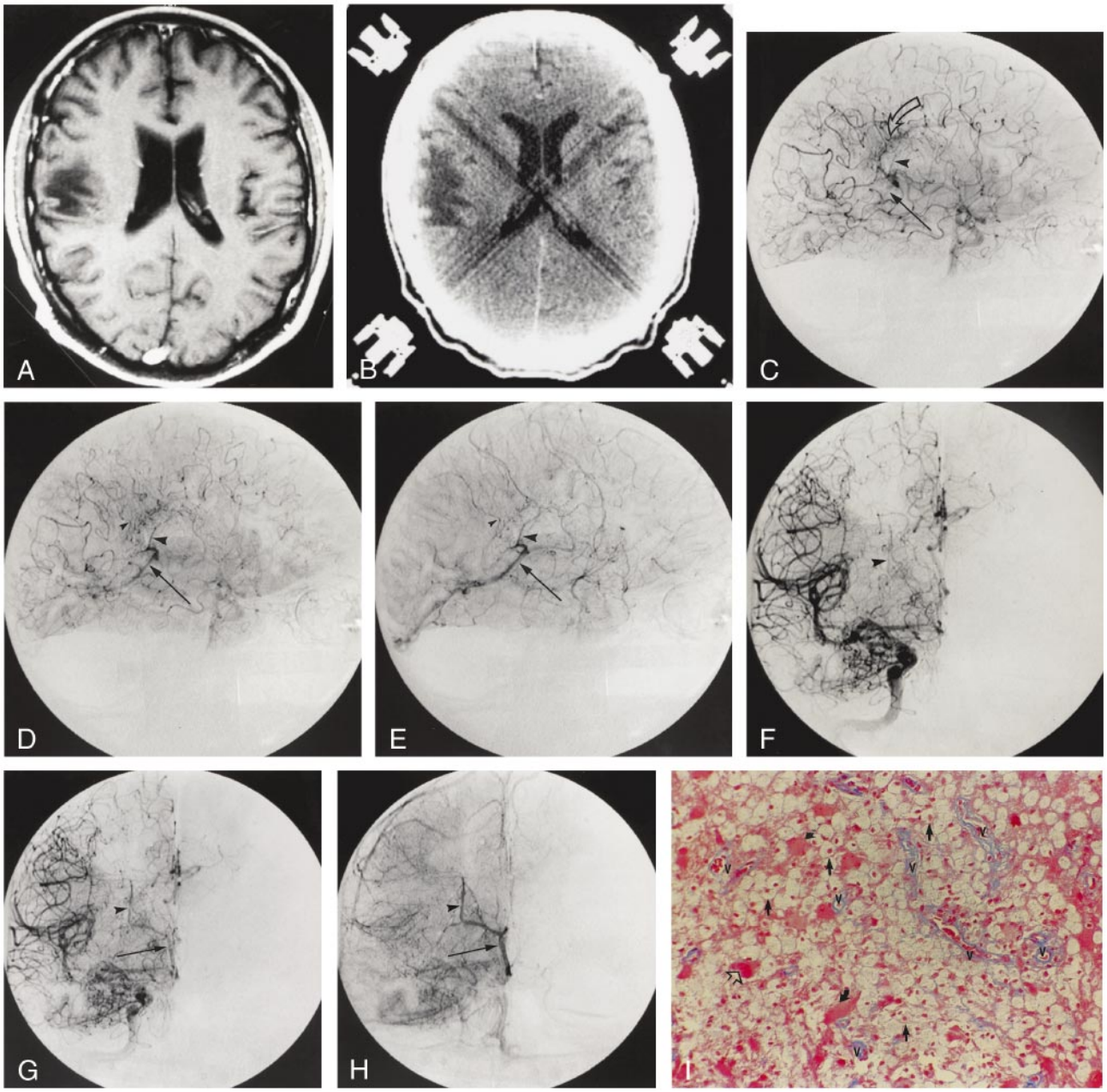

FIG 2. Patient 2.

A, Contrast-enhanced T1-weighted MR image (600/14/2) illustrates the nonenhancing right posterior frontal lesion.

B, Corresponding contrast-enhanced CT scan shows a hypodense deep and subcortical white matter lesion.

C–E, Late arterial (*C*), capillary (*D*), and early venous (*E*) phase digital subtraction angiographic (DSA) images (lateral projection) from the accompanying right internal carotid artery (ICA) angiogram depict a region of arteriovenous shunting corresponding to the location of the MR abnormality. A dense parenchymal blush is evident throughout the inferior frontoparietal region (*curved arrow, C*). Arteriovenous shunting results in the early opacification of a direct atrial vein (*large arrowhead*) and the posterior third of the right internal cerebral vein (*arrow*). An early draining cortical parietal vein is seen in *D* and *E* (*small arrowhead*).

F–H, Corresponding mid-arterial (*F*), late arterial (*G*), and early venous (*H*) phase frontal DSA images confirm early opacification of the atrial (*arrowhead*) and right internal cerebral (*arrow*) veins.

I, Histologic section shows several vascular channels (*v*) without evidence of reduplication of the basal lamina. There is mingling of numerous histiocytes (*straight arrows*) and reactive astrocytes (*curved arrows*), characteristic of a demyelinating process. Some of the astrocytic cells have enlarged hyperplastic nuclei (*open arrows*) often seen in PML (azocarmine stain, original magnification ×100).

variable extent in all cases. In patient 1, who had enhancement of the focus of PML in the posterior fossa, the inflammatory perivascular cuffing was most pronounced (Fig 1G and H). This was accompanied by plumping of the endothelial cells (Fig 1H) and fragmentation of the matrix protein of the basal lamina (Fig 1I), which was not identified in the other cases. Conversely, the two patients with angiographically occult lesions (cases 5 and 6) had the most ordinary findings histologically, with minimal perivascular inflammatory reaction, angiogenesis, and gliosis (Fig 4). No other CNS infectious

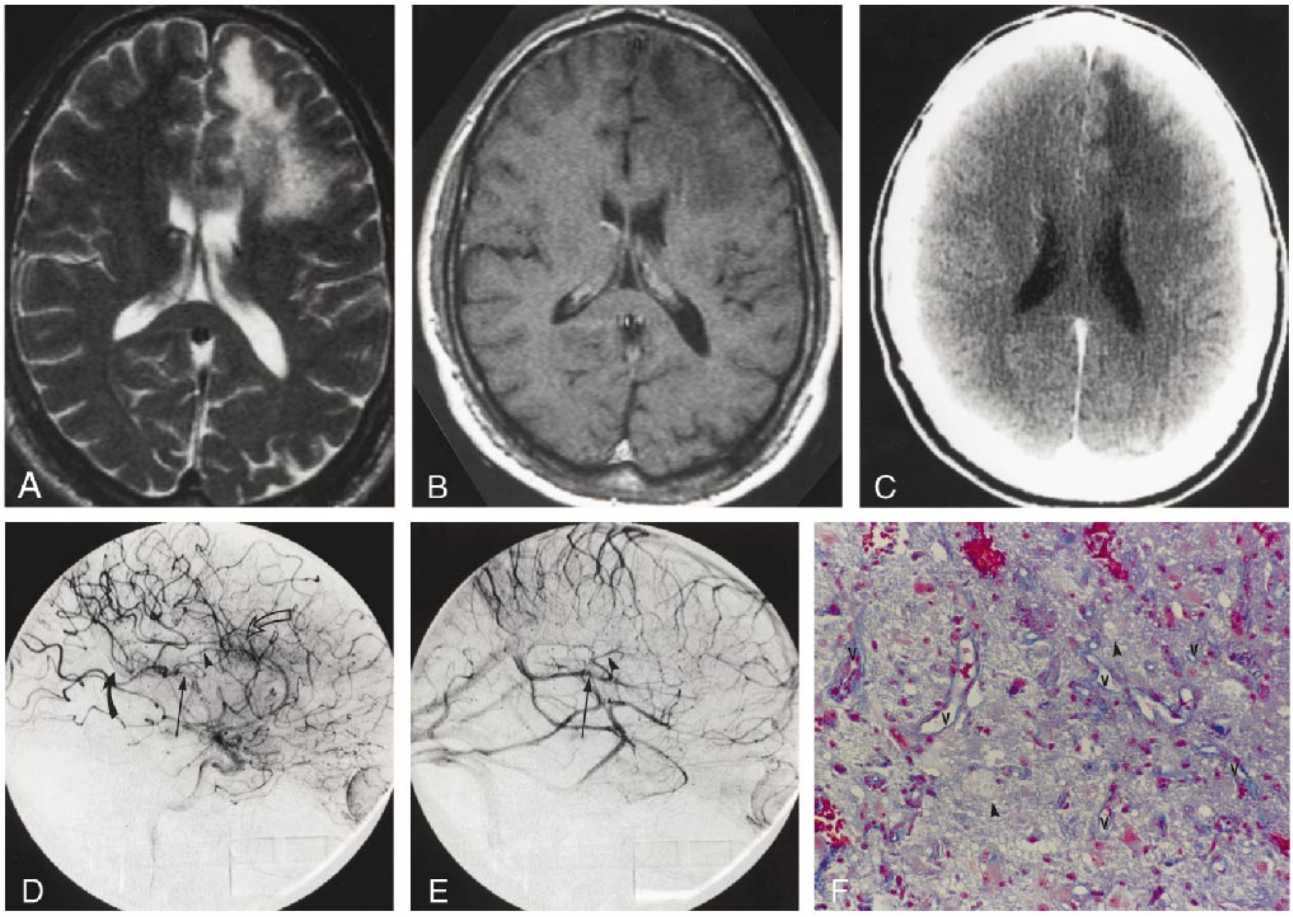

FIG 3. Patient 3.

A and *B,* Axial T2-weighted (3400/119/1) (*A*) and contrast-enhanced T1-weighted (600/14/2) (*B*) MR images show the nonenhancing left frontal lesion.

C, Corresponding contrast-enhanced CT scan shows a nonenhancing hypodense white matter lesion.

D and *E,* Arterial (*D*) and venous (*E*) phase DSA images (lateral projection) from the accompanying left ICA stereo angiogram depict a region of arteriovenous shunting corresponding to the location of the MR abnormality. An area of abnormal parenchymal blush (*curved open arrow*) is associated with arteriovenous shunting, resulting in the early opacification of an anterior caudate vein (*arrowhead*), which empties via the thalamostriate trunk into the left internal cerebral vein (*straight arrow*). Contrast within the vein of Galen is identified during the arterial phase (*curved solid arrow, D*).

F, Histopathologic specimen from the region of abnormal parenchymal blush and arteriovenous shunting show numerous small vascular channels (*v*) outlined by azocarmine. The neuropile (*arrowheads*) is rarified (azocarmine stain, original magnification ×100).

or neoplastic processes were identified pathologically in any of the patients.

Discussion

The presence of structural and/or functional microvascular changes within lesions of the CNS can be inferred from the identification of angiographic abnormalities (arteriovenous shunting and parenchymal blush) and abnormal contrast enhancement on CT or MR studies, despite the often unclear pathologic substrate for these alterations. In the past, PML has been described as angiographically occult; however, among a group of six patients with pathologically proved PML, we observed four cases of lesion-related arteriovenous shunting. With one exception these lesions failed to enhance on CT or MR studies. We hoped to gain some insight into the pathophysiological derangements in the cerebral vasculature responsible for these angiographic abnormalities by analyzing the histologic specimens in the context of the angiographic and cross-sectional imaging appearances.

Oligodendrocytes are responsible for the formation and maintenance of myelin sheaths in the CNS. PML develops after infection of these oligodendrocytes by the JC virus, and is characterized pathologically by intranuclear inclusions in oligodendrocytes, bizarre astrocytes, foamy macrophages, and foci of demyelination (which may become extensive and confluent) (1, 6). In advanced cases, areas of frank necrosis may occur. Asymmetric involvement of both cerebral hemispheres is typical; extension to the basal ganglia and deep layers of the cerebral cortex is also seen. In the posterior fossa, PML can affect the granular cell layer and white matter of the cerebellum and the white matter tracts of the brain stem (1, 6–8).

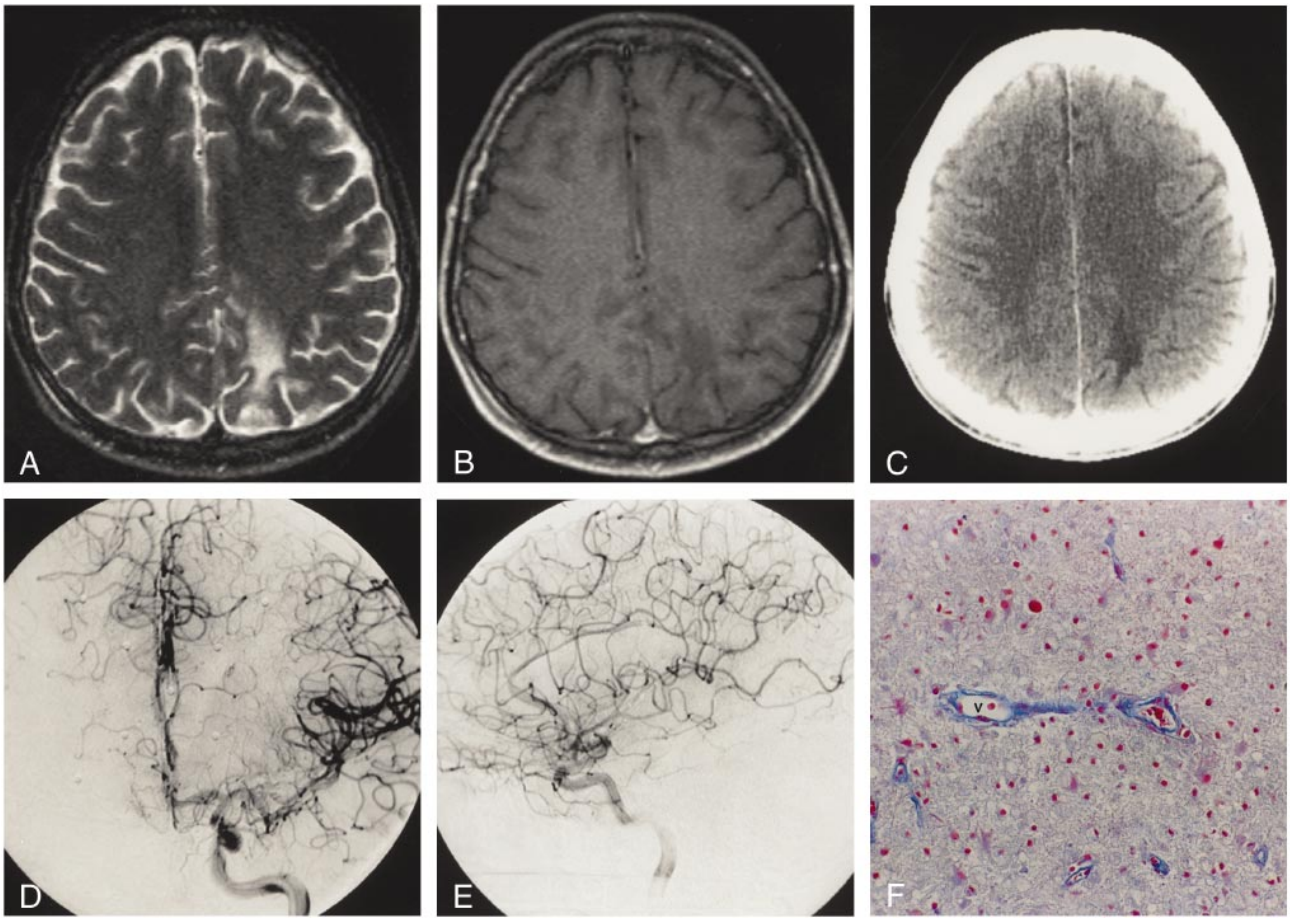

FIG 4. Patient 5.

A and *B,* Axial T2-weighted (3400/119/1) (*A*) and contrast-enhanced T1-weighted (600/14/2) (*B*) MR images show a nonenhancing left parietal focus of PML.

C, Accompanying contrast-enhanced CT scan shows a nonenhancing hypodensity in the white matter of the left parietal lobe.

D and *E,* Anteroposterior (*D*) and lateral (*E*) arterial phase DSA images from the left ICA stereo angiogram fail to show any abnormal parenchymal blush or evidence of arteriovenous shunting.

F, A vascular channel (*v*) devoid of perivascular inflammation is outlined by azocarmine, illustrating the ordinary histologic appearance in this patient with an angiographically occult lesion (azocarmine stain, original magnification ×100).

There are differences in the spectrum of neuropathologic findings between AIDS and non-AIDS–associated PML. A number of authors have identified more extensive foci of demyelination, as well as more prominent and extensive perivascular mononuclear inflammatory infiltrates in HIV-positive patients (1, 6, 9). Kuchelmeister et al (1) described three cases of inflammatory infiltrates within vessel walls in AIDS-associated cases. Conversely, in cases of non-AIDS–associated PML, perivascular infiltrates have generally been minimal or absent (2, 3).

On CT scans, PML characteristically appears as a hypodense lesion without edema, mass effect, or contrast enhancement, and often with scalloped margins at the gray/white junction (reflecting involvement of subcortical U fibers) (7, 10–13) (Fig 2B). On MR examinations (which are much more sensitive for lesion detection) PML is hyperintense relative to normal white matter on long TR/TE sequences, hypointense on short TR/TE images, and usually fails to enhance after intravenous administration of contrast material (7, 14) (Figs 2–4). Although uncommon, exceptions to this typical pattern of nonenhancing lesions are well described, with faint rim enhancement occasionally identified on both CT and MR studies (6, 7, 11, 13) (Fig 1).

Angiographic findings have been described in a small number of cases (mostly in patients with non-AIDS–associated PML). In these reports, foci of PML have generally been avascular (10, 15, 16), although in two patients (one with systemic lupus erythematosus and the other with Hodgkin disease) arteriovenous shunting was described, in one of which there was an associated abnormal parenchymal blush (17, 18). Faint blushes with nonspecific dilatation of small arteries and medullary veins have also been reported in several cases (10–12). We identified abnormal angiographic findings in four of our six patients. In each case, the abnormality was characterized by a pathologic parenchymal blush and arteriovenous shunting (Figs 1–3).

The presence of a pathologic blush or stain at cerebral angiography typically reflects the aggre-

gate size and density of small vessels within the domain of the lesion defined by the blush. Such angiographic changes may be seen in primary and secondary brain neoplasms in which a focal pathologic increase in vascular density, accompanied by features of angiogenesis, occurs in response to specific cytokines (including vascular endothelial growth factor and basic fibroblast growth factor) elaborated by the tumor cells (19). Arteriovenous shunting (manifest angiographically by an accelerated vascular transit time) accompanies a reduction in the resistance of a discrete vascular territory relative to the surrounding brain parenchyma, and may reflect structural or functional alterations to the cerebral vasculature. Structural (anatomic) arteriovenous shunting occurs in arteriovenous malformations and in conditions associated with angiogenesis (such as tumors, inflammation/infection), particularly if the newly elaborated vessels exhibit autoregulatory incompetence. Functional (physiological) arteriovenous shunting, due to impaired autoregulation, may develop independently in response to conditions of local cerebral hypoxia/acidosis, and is related to a decrease in vascular resistance caused by vasodilation of small arteries and arterioles. In certain pathologic states (eg, parenchymal tumors and some inflammatory processes), both processes may contribute to the development of arteriovenous shunting with individual autocoids (such as kinins and eicosanoids) (20) and/or cytokines acting separately to cause vasodilatation and promote angiogenesis.

Considering the pathologic changes observed in our patients with PML, the presence of angiographic abnormalities is not unexpected. We observed an increase in small-vessel density (due to neoangiogenesis) in biopsy specimens from all patients with lesion-related arteriovenous shunting. In addition, regions of robust inflammatory change, characterized by the diffuse presence of macrophages and lymphocytes, were present in all four patients with arteriovenous shunting. The two patients with angiographically occult lesions (cases 5 and 6) were the only ones to not have significant neovascularization or inflammatory infiltration (Fig 4).

Although, as with intracranial neoplasms, neoangiogenesis may account for the angiographic abnormalities observed in our patients, secondary functional mechanisms may also play a role. The presence of active inflammation is likely to result in the elaboration of vasoactive substances that potentially could alter vasomotor tone within the lesion, decreasing local angiographic transit time through vasodilatory effects on small arteries and arterioles and increasing the parenchymal staining characteristics of the lesion through vasodilation of small venules. Moreover, the release of certain kininlike substances or eicosanoids may alter the permeability of the blood-brain barrier locally, leading to contrast enhancement on CT or MR examinations.

Contrast enhancement of parenchymal lesions on CT or MR studies occurs primarily as a result of derangement of the blood-brain barrier (21). Neovascularization may also play a role (22). In the one patient (case 1) in this series in whom the focus of PML enhanced on MR images, there were distinctive neuropathologic findings. Not only was there a florid perivascular inflammatory infiltrate but also infiltration of the vessel walls themselves by inflammatory cells together with fragmentation of the basal lamina (Fig 1G–I). Such changes were not observed in any of the other patients, suggesting a distinct relationship between the unique microvascular inflammatory changes found in this lesion and its contrast-enhancing characteristics on MR images.

A potential criticism of our data is that the neuropathologic findings on the biopsy material might not be representative of those in other parts of the lesion (ie, sampling error). We think that this is unlikely, as in each patient, three to six specimens were obtained, with the stereotactic coordinates for each specimen determined from the cross-sectional imaging studies.

Conclusion

The high prevalence of angiographic abnormalities in our series (66% of patients) is in marked distinction to that described previously. We believe that this is a reflection of our patient population, all of whom had AIDS, and of changes characterized by angiogenesis and perivascular inflammation. The pathologic parenchymal blush and arteriovenous shunting seen angiographically reflect the capillary proliferation and perivascular inflammatory changes incited by the presence of the JC virus in infected oligodendrocytes.

References

1. Kuchelmeister K, Gullotta F, Bergmann M, Angeli G, Masini T. **Progressive multifocal leukoencephalopathy (PML) in the acquired immunodeficiency syndrome (AIDS).** *Pathol Res Pract* 1993;189:163–173
2. Astrom K-E, Mancall EL, Richardson EP. **Progressive multifocal leuko-encephalopathy: a hitherto unrecognized complication of chronic lymphatic leukaemia and Hodgkin's disease.** *Brain* 1958;81:93–111
3. Richardson EP. **Progressive multifocal leukoencephalopathy.** *N Engl J Med* 1961;265:815–823
4. Richardson EP. **Progressive multifocal leukoencephalopathy 30 years later.** *N Engl J Med* 1988;318:315–317
5. Berger JR, Kaszovitz B, Post JD, Dickinson G. **Progressive multifocal leukoencephalopathy associated with human immunodeficiency virus infection.** *Ann Intern Med* 1987;107:78–87
6. von Einsiedel RW, Fife TD, Aksamit AJ, et al. **Progressive multifocal leukoencephalopathy in AIDS: a clinicopathologic study and review of the literature.** *J Neurol* 1993;240:391–406
7. Whiteman MLH, Post MJD, Berger JR, Tate LG, Bell MD, Limonte LP. **Progressive multifocal leukoencephalopathy in 47 HIV-seropositive patients: neuroimaging with clinical and pathologic correlation.** *Radiology* 1993;187:233–240
8. Sweeney BJ, Miller RF, Harrison MJG. **Progressive multifocal leucoencephalopathy.** *Br J Hosp Med* 1993;50:187–192
9. Aksamit AJ, Gendelman HE, Orenstein JM, Pezeshkpour GH. **AIDS-associated progressive multifocal leukoencephalopathy: comparison to non-AIDS PML with in situ hybridization and immunohistochemistry.** *Neurology* 1990;40:1073–1078

10. Carroll BA, Lane B, Norman D, Enzmann D. **Diagnosis of progressive multifocal leukoencephalopathy by computed tomography.** *Radiology* 1977;122:137–141
11. Heinz ER, Drayer BP, Haenggeli CA, Painter MJ, Crumrine P. **Computed tomography in white-matter disease.** *Radiology* 1979;130:371–378
12. Krupp LB, Lipton RB, Swerdlow ML, Leeds NE, Llena J. **Progressive multifocal leukoencephalopathy: clinical and radiographic features.** *Ann Neurol* 1985;17:344–349
13. Wheeler AL, Truwit CL, Kleinschmidt-DeMasters BK, Byrne WR, Hannon RN. **Progressive multifocal leukoencephalopathy: contrast enhancement on CT scans and MR images.** *AJR Am J Roentgenol* 1993;161:1049–1051
14. Mark AS, Atlas SW. **Progressive multifocal leukoencephalopathy in patients with AIDS: appearance on MR images.** *Radiology* 1989;173:517–520
15. Conomy JP, Beard NS, Matsuoto H, Roessmann U. **Cytarabine treatment of progressive multifocal leukoencephalopathy.** *JAMA* 1974;229:1313–1316
16. Jones HR, Hedley-Whyte ET, Freidberg SR, Kelleher JE, Krolikowski J. **Primary cerebellopontine progressive multifocal leukoencephalopathy diagnosed premortem by cerebellar biopsy.** *Ann Neurol* 1982;11:199–202
17. Cunningham ME, Kishore PRS, Rengachary SS, Preskorn S. **Progressive multifocal leukoencephalopathy presenting as focal mass lesion in the brain.** *Surg Neurol* 1977;8:448–450
18. Tomura N, Watanabe M, Kato T, Nishino K, Kowada M. **Case report: progressive multifocal leukoencephalopathy with prominent medullary veins on angiogram.** *Clin Radiol* 1994;49: 66–68
19. Zagzag D. **Angiogenic growth factors in neural embryogenesis and neoplasia.** *Am J Pathol* 1995;146:293–309
20. Serafin WE, Babe KS Jr. **Autocoids: drug therapy of inflammation.** In: Hardman JG, Limbird LE, eds. *Goodman and Gilman's The Pharmacologic Basis of Therapeutics.* 9th ed. New York: McGraw-Hill; 1996:579–580
21. Sage MR, Wilson AJ. **The blood-brain barrier: an important concept in neuroimaging.** *AJNR Am J Neuroradiol* 1994;15:601–622
22. Zagzag D, Goldenberg M, Brem S. **Angiogenesis and blood-brain barrier breakdown modulate CT contrast enhancement: an experimental study in a rabbit brain-tumor model.** *AJNR Am J Neuroradiol* 1989;10:529–534